The First Anionic Sulfonamide-Binding Zinc(II) Complexes with a Macrocyclic Triamine: Chemical Verification of the Sulfonamide Inhibition of Carbonic Anhydrase

Tohru Koike,[†] Eiichi Kimura,*[,†] Ikushi Nakamura,[†] Yukie Hashimoto,[†] and Motoo Shiro[‡]

Contribution from the Department of Medicinal Chemistry, School of Medicine, Hiroshima University, Kasumi 1-2-3, Minami-ku, Hiroshima 734, Japan, and Rigaku Corporation, Matsubaracho 3-9-12, Akishima, Tokyo 196, Japan. *Received March 10, 1992*

Abstract: A zinc(II) complex with 1-(3-(*p*-toluenesulfonamido)propyl)-1,5,9-triazacycloundecane ("tosylamidopropyl[12]aneN$_3$", L_2), **2a**, has been synthesized as a model for sulfonamide inhibition of carbonic anhydrase (CA). X-ray crystal structure analysis of **2a** showed a distorted tetrahedral structure, where a strong interaction is revealed between Zn^{II} and the sulfonamide N^- anion (1.925 (3) Å). Crystals of **2a**·PF_6 ($C_{19}H_{33}N_4O_2F_6PSZn$) are orthorhombic, space group *Pbca* with a = 17.508 (4) Å, b = 15.394 (4) Å, c = 18.377 (5) Å, V = 4953 (4) Å^3, and Z = 8. A full-matrix least-squares refinement yielded R = 0.040 and R_w = 0.056 for 2862 independent reflections. Potentiometric titrations of L_2 and Zn^{II} disclosed extremely facile deprotonation of the sulfonamide group at pH < 7 and 25 °C to bind to Zn^{II} in the 12-membered macrocyclic triamine complex. This intramolecular sulfonamide N^- binding to Zn^{II} completely inhibits formation of the Zn^{II}–OH^- species, which, as a model for CA active site, was previously shown to be formed with [12]aneN$_3$ at pH ~ 7 and possess a strong nucleophilicity in ester hydrolysis or acetaldehyde hydration. The new complex **2a** has no activity in 4-nitrophenyl acetate hydrolysis. Thus, **2a** is shown to be a good chemical model for the strong sulfonamide inhibition of CA. Intermolecular interaction of the Zn^{II}–[12]aneN$_3$ complex **1a** with HCO_3^- (a CA substrate), *p*-toluenesulfonamide, 4-nitrobenzenesulfonamide, and acetazolamide (a most potent CA inhibitor) was quantitatively determined by inhibition kinetics in 4-nitrophenyl acetate hydrolysis. The intermolecular inhibition (due to decrease in concentration of Zn^{II}–L_1–OH^- **1b**) was caused by Zn^{II}–L_1–$ArSO_2NH^-$ **1c** or –HCO_3^- **1d** formation and the inhibition order was acetazolamide (log K_i = 3.6) > HCO_3^- (2.8) > 4-nitrobenzenesulfonamide (2.6) > *p*-toluenesulfonamide (2.4). The apparent sulfonamide affinities (K_i at pH 8.4) to **1a** are parallel with those reported for CA, and thus our model study provides the first chemical evidence of strong acetazolamide-binding to Zn^{II} in CA.

Introduction

Catalytic mechanisms of zinc-containing carbonic anhydrases (CA) consistently have been interesting bioinorganic subjects.[1] Most of the strong CA inhibitors are anions (e.g., SCN^-, CN^-, I^-), inhibition by which is understandable in light of the known enzyme–substrate complex formed between CA and anionic HCO_3^-. On the other hand, neutral sulfonamides (e.g., acetazolamide ("Haa"), *p*-toluenesulfonamide ("Hts"), 4-nitrobenzenesulfonamide ("Hns"), etc.) are even stronger inhibitors of CA.[2-4] On the basis of spectroscopic studies[2d,g] and X-ray crystallographic analyses (with CA–acetazolamide at 3 Å resolution and with CA–3-(acetoxymercurio)-4-aminobenzenesulfonamide at 2 Å resolution),[3] it is now accepted that sulfonamides bind to Zn^{II} as unidentate anions (e.g., aa^-, ts^-, ns^-) in a hydrophobic pocket of the CA active center (Scheme I).[2] However, due to the lack of appropriate chemical models, some intrinsic questions remain unanswered: (i) do sulfonamides intrinsically bind to Zn^{II} as anions; (ii) how much are the pK_a values of the sulfonamides lowered by binding to Zn^{II}; (iii) does sulfonamide anion binding to the Zn^{II} really cause the loss of the Zn^{II} acidity that is the essence of CA activity; and (iv) is the hydrophobic environment indeed necessary for sulfonamide binding to CA?

Recently, we discovered that a zinc(II) complex (**1a** and **b**) with a tridentate ligand, 1,5,9-triazacyclododecane ([12]aneN$_3$), L_1, is structurally as well as dynamically the best model for the role of Zn^{II} in CA[5] and zinc(II)-containing phosphatase enzymes.[6]

Scheme I

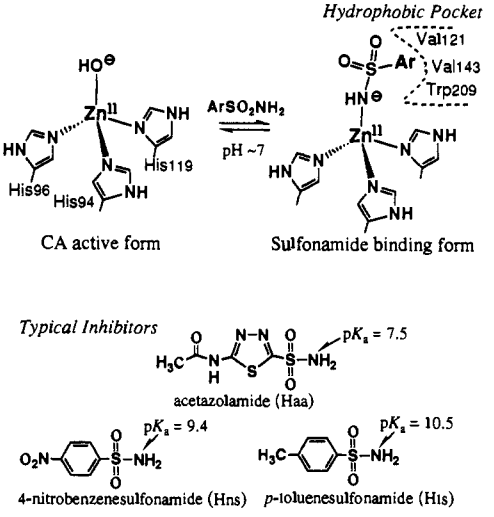

† Hiroshima University.

‡ Rigaku Corporation.

(1) (a) Lindoskog, S. In *Zinc Enzymes*, Brikäuser: Boston, MA, 1986; Chapter 22, p 307. (b) Eriksson, E. A.; Jones, T. A.; Liljas, A. In *Zinc Enzymes*; Chapter 23, p 317. (c) Sen, A. C.; Tu, C. K.; Thomas, H.; Wynns, G. C.; Sylverman, D. N. In *Zinc Enzymes*; Chapter 24, p 329. (d) Pocker, Y.; Janjic, N.; Miao, C. H. In *Zinc Enzymes*; Chapter 25, p 341. (e) Khalifah, R. G.; Rogers, J. I.; Mukherjee, J. In *Zinc Enzymes*; Chapter 26, p 357. (f) Bertini, I.; Luchinat, D. C.; Monnanni, R. In *Zinc Enzymes*; Chapter 27, p 371.

(2) (a) Taylor, P. W.; King, R. W.; Burgen, A. S. V. *Biochemistry* **1970**, *9*, 2638. (b) Taylor, P. W.; King, R. W.; Burgen, A. S. V. *Biochemistry* **1970**, *9*, 3894. (c) Liang, Jiin-Y.; Lipscomb, W. N. *Biochemistry* **1989**, *28*, 9724. (d) King, R. W.; Burgen, A. S. V. *Biochim. Biophys. Acta* **1970**, *207*, 278. (e) Binford, J. S.; Lindskog, S.; Wadsö, I. *Biochim. Biophys. Acta* **1974**, *341*, 345. (f) Vedani, A.; Dunitz, J. D. *J. Am. Chem. Soc.* **1985**, *107*, 7653. (g) Kanamori, K.; Roberts, J. D. *Biochemistry* **1983**, *22*, 2658. (h) King, R. W.; Burgen, A. S. V. *Prov. R. Soc. London, B* **1976**, *193*, 107.

(3) Eriksson, A. E.; Kylsten, Per M.; Jones, T. A.; Liljas, A. *Proteins* **1988**, 283.

(4) In the course of the preparation of this manuscript a two deprotonated acetazolamide binding complex, Zn^{II}–$(aa^-)_2(NH_3)_2$ was reported: Hartmann, U.; Vahrenkamp, H. *Inorg. Chem.* **1991**, *30*, 4676. However, little thermodynamic or kinetic implication of the CA–acetazolamide interaction was deduced, other than the fact that acetazolamide may be deprotonated to bind with Zn^{II}.

(5) (a) Kimura, E.; Shiota, T.; Koike, T.; Shiro, M.; Kodama, M. *J. Am. Chem. Soc.* **1990**, *112*, 5805. (b) Kimura, E.; Koike, T. *Comments Inorg. Chem.* **1991**, *11*, 285. (c) Kimura, E.; Koike, T.; Toriumi, K. *Inorg. Chem.* **1988**, *27*, 3687. (d) Kimura, E.; Koike, T.; Shiota, T.; Iitaka, Y. *Inorg. Chem.* **1990**, *29*, 4621.

(6) Koike, T.; Kimura, E. *J. Am. Chem. Soc.* **1991**, *113*, 8937.

0002-7863/92/1514-7338$03.00/0

The zinc(II) hydroxide complex **1b** catalyzes the hydration of acetaldehyde and hydrolysis of acetate,[5a] both of which are also catalyzed by CA. Although we have observed acetazolamide anion binding to Zn^{II}–[12]aneN$_3$ complex, **1c** (D = aa$^-$), the isolated microcrystalline products were not suitable enough for X-ray crystal study.[5a] We then suspected that an intramolecularly

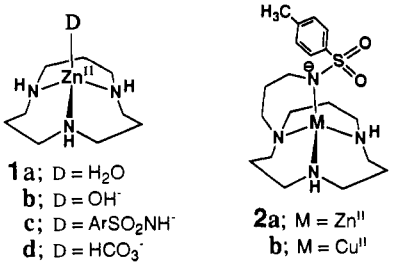

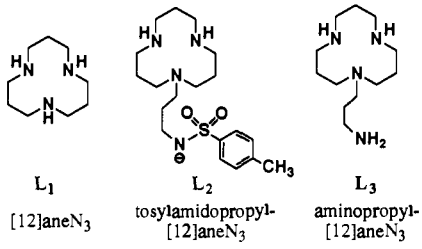

attached tosylamide in 1-(3-(*p*-toluenesulfonamido)propyl)-1,5,9-triazacyclododecane ("tosylamidopropyl[12]aneN$_3$", **L$_2$**) might make a better model **2a**, that might further serve to bridge the enzymological facts with the chemical evidence for sulfonamide anion binding to Zn^{II}. To elucidate the specific character of the fourth coordination site for sulfonamide anions in **2**, we also investigated the coordination chemistry of the parent macrocyclic polyamine with a neutral "aminopropyl[12]aneN$_3$", **L$_3$**.

The interaction of sulfonamides (CA inhibitors; Haa, Hts, and Hns) and HCO$_3^-$ (a CA substrate) with Zn^{II}–[12]aneN$_3$ was determined by studying their inhibitory effect on 4-nitrophenyl acetate (NA) hydrolysis promoted by **1b** (Scheme II). The results

Scheme II

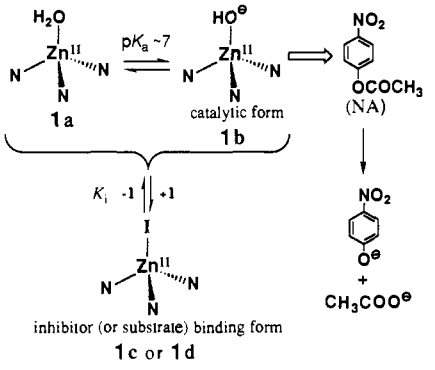

Scheme III

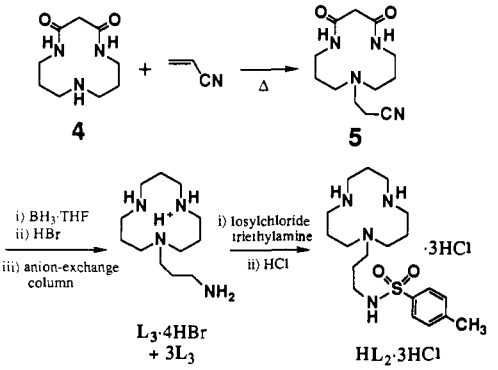

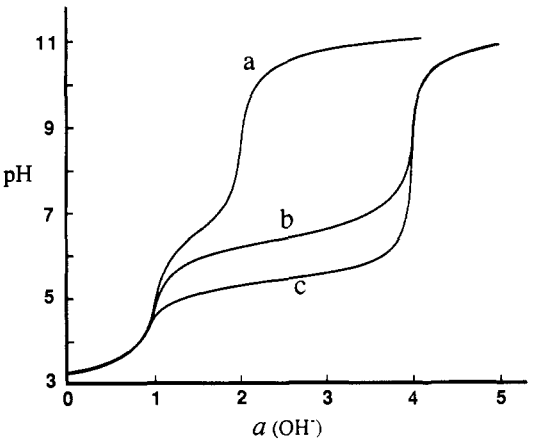

Figure 1. pH titration curves for HL$_2$·3H$^+$ at I = 0.10 (NaClO$_4$) and 25 °C: (a) 1.00 mM HL$_2$·3H$^+$; (b) solution a + 1.00 mM Zn^{II}SO$_4$; and (c) solution a + 1.00 mM Cu^{II}SO$_4$. a(OH$^-$) is the moles of base (NaOH) per mole of ligand.

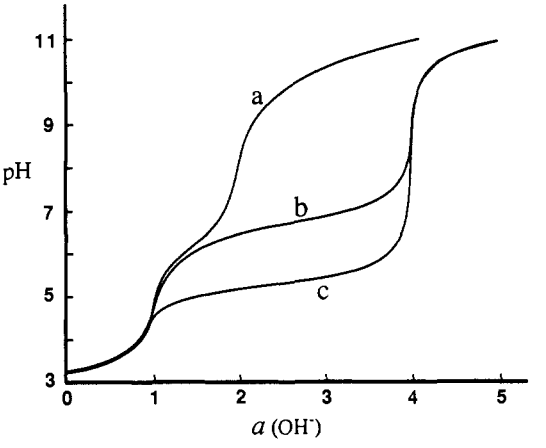

Figure 2. pH titration curves for L$_3$·4H$^+$ at I = 0.10 (NaClO$_4$) and 25 °C: (a) 1.00 mM L$_3$·4H$^+$; (b) solution a + 1.00 mM Zn^{II}SO$_4$; and (c) solution a + 1.00 mM Cu^{II}SO$_4$. a(OH$^-$) is the moles of base (0.10 M NaOH) per mole of ligand.

Table I. Protonation Constants K_n[a] and Zn^{II} and Cu^{II} Complex Formation Constants K(ML)[b] for 12-Membered Macrocyclic Triamines at 25 °C and I = 0.10 (NaClO$_4$)

	L$_1$	L$_2$	L$_3$
log K_1	12.60[c]	12.2 ± 0.1	12.1 ± 0.1
log K_2	7.57[c]	11.23 ± 0.03	10.01 ± 0.03
log K_3	2.41[c]	6.40 ± 0.02	6.10 ± 0.02
log K_4		2.75 ± 0.05	2.3 ± 0.1
log K(Zn^{II}L)	8.4[d] (8.7)[c]	14.7 ± 0.1	11.7 ± 0.1
log K(Cu^{II}L)	12.6[c]	16.9 ± 0.1	16.0 ± 0.1

[a] K_n = [H$_n$L]/[H$_{n-1}$]·a_{H^+}. [b] K(ML) = [ML]/[M][L]. [c] From ref 8 at I = 0.1 (KNO$_3$) and 25 °C. [d] From ref 5a at I = 0.1 (NaClO$_4$) and 25 °C.

presented here indeed show strong coordination of the inhibitors and substrate (I as anionic species) to Zn^{II} of **1**. Moreover, the apparent sulfonamide affinity constants (K_i) almost parallel those previously reported for CA.[2a]

Results and Discussion

New Ligands, L$_2$ and L$_3$, and Protonation Constants. The target ligand **L$_2$** and the intermediate **L$_3$** were synthesized from macrocyclic dioxotriamine **4**[7] and acryronitrile (Scheme III). Since the two secondary amines of **L$_3$** are fairly sensitive to tosyl chloride, selective protection of the macrocyclic NH groups as a monoprotonated [12]aneN$_3$ by mixing of 3:1 acid-free **L$_3$** and L$_3$·4HBr

(7) Helps, I. M.; Parker, D.; Jankowski, K. J.; Chapman, J.; Nicholson, P. E. *J. Chem. Soc., Perkin Trans. I* **1989**, 2079.

Scheme IV

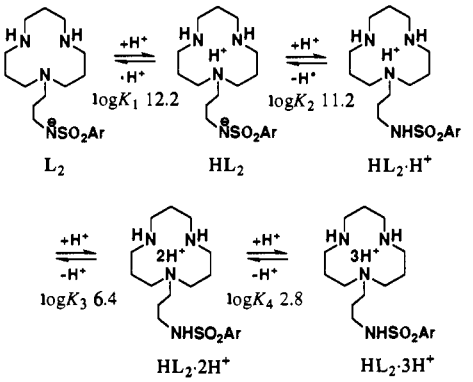

was conducted to get a monotosylated ligand, HL_2, in 77% yield.

The protonation constants (K_n) of L_2 and L_3 were determined by potentiometric pH titrations at $I = 0.10$ ($NaClO_4$) and 25 °C (Figures 1a and 2a). Table I summarizes the protonation constants as logarithmic values in comparison with the reported K_n values of L_1.[8]

For tosylamidopropyl[12]aneN$_3$, L_2, the four protonation constants K_1–K_4 are assigned as in Scheme IV. This assignment comes from the following facts: (i) the pendantless [12]aneN$_3$, L_1, has an extremely large protonation constant, log K_1 of 12.6, while the remaining two are 7.57 and 2.41 (see Table I);[8] (ii) a protonation constant of the tosylamide anion of L_2, log K = 11.2 ± 0.1 was derived from the 227-nm absorption change ($\epsilon = 1.08 \times 10^4$ for the anionic form at pH 12.5 and 1.65×10^4 for the neutral form at pH 9.0) at $I = 0.10$ ($NaClO_4$) and 25 °C;[9] (iii) ^{1}H NMR-pD titration of L_2 (in D_2O at 25 °C) disclosed the first protonation constant, log K_1 = 12.5 ± 0.2 is assigned to the macrocyclic nitrogen atoms, while the second one, log K_2 = 11.7 ± 0.2 to the sulfonamide group (see Experimental Section). By drawing an analogy, the second protonation constant of L_3, log K_2 = 10.01 ± 0.03, was assigned to the pendant primary amine as shown below, and the remaining values log K_1 = 12.1 ± 0.1, log K_3 = 6.10 ± 0.02, and log K_4 = 2.3 ± 0.1 to the macrocyclic triamine moiety. From the protonation constants for the pendant donors, deprotonation of the primary ammonium group in L_3 is ca. 16 times easier than that of the sulfonamide in L_2.

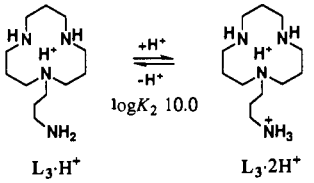

Zinc(II) and Copper(II) Complexes with L_2 and L_3. The Zn^{II} and Cu^{II} complexation equilibria for L_2 and L_3 were determined by 0.1 M NaOH titration of 1 mM of completely protonated ligands $HL_2 \cdot 3H^+$ (Figure 1b,c) and $L_3 \cdot 4H^+$ (Figure 2b,c) in the presence of equivalent $ZnSO_4$ or $CuSO_4$. The smooth buffer curves with L_2 do not break until four protons are neutralized at $a(OH^-) = 4$, implying that the Zn^{II} and Cu^{II} complexations do not halt at the stage of M–OH_2 complexes MHL_2 **6** but go further to neutralization of one more proton (Scheme V). The expected candidate products are ML_2 **2** and/or **7**. Another unlikely route to sulfonamide hydrolysis by nucleophilic attack from Zn^{II}-bound OH^- of **7** was not observed at all. Evidence for the sulfonamide deprotonated complex structure **2** comes from the asymmetric SO_2 stretching frequency ($\nu_{as}SO_2$) changes (in pH 8 aqueous solution) from 1310 cm^{-1} of the metal-unbinding ligand $HL_2 \cdot H^+$ to 1230 cm^{-1} for **2a** and **2b**, which is assignable to the deprotonated

Scheme V

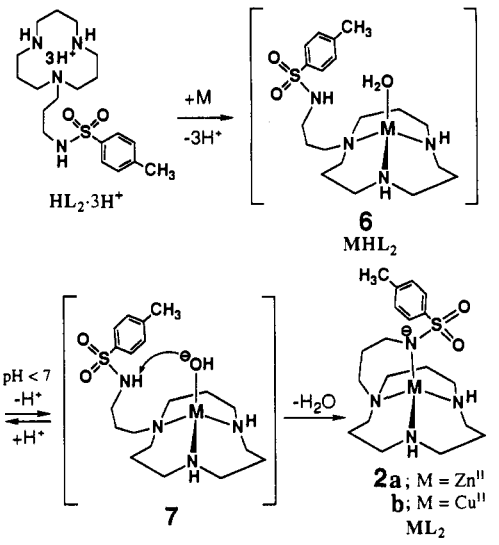

sulfonamide group.[10] More concrete evidence for the structure **2a** is derived from an X-ray analysis of the Zn^{II} complex **2a**·PF_6 isolated from pH 7.5 aqueous solution (see next paragraph). We also synthesized **2b**·BPh_4 as fine green crystals from aqueous solutions of the 1:1 Cu^{II} and L_2 in the presence of excess $NaBPh_4$. In the solid state the $\nu_{as}SO_2$ value of 1323 cm^{-1} for $HL_2 \cdot 3HCl$ shifts to lower wave numbers of 1263 cm^{-1} for **2a**·PF_6 and 1267 cm^{-1} for **2b**·BPh_4.

From the analysis of the titration data at $I = 0.10$ ($NaClO_4$) and 25 °C, the complexes **2a** and **2b** formation constants, log K(ML) of 14.7 ± 0.1 and 16.9 ± 0.1, respectively, were determined (see eq 1). The values are much larger than those for pendantless [12]aneN$_3$ complex Zn^{II}–L_1 (log $K(Zn^{II}L)$ = 8.4) and for Cu^{II}–L_1 (log $K(Cu^{II}L)$ = 12.6) (see Table I).

$$M + L \rightleftharpoons ML \qquad K(ML) = [ML]/[M][L]\ (M^{-1}) \quad (1)$$

Complexation of L_3 with Zn^{II} and Cu^{II} occurred smoothly (at $1 < a(OH^-) < 4$ of Figure 2b,c) to form ML_3 **3**. More interestingly, Zn^{II}– and Cu^{II}–L_3 complexes **3a** (log $K(Zn^{II}L)$ = 11.7) and **3b** (log $K(Cu^{II}L)$ = 16.0) are less stable than those of L_2, **2a** (14.7), and **2b** (16.9). Namely, the sulfonamide N$^-$ anion is a stronger donor than either the parent neutral amino group or water. Furthermore, the sulfonamidopropyl pendant N$^-$ anion has a greater stabilizing effect on the Zn^{II} complex than on the Cu^{II} complex, as disclosed by comparison of their respective formation constant ratios, $K(ML_2)/K(ML_3) = 10^3$ for M = Zn^{II} vs $10^{0.9}$ for M = Cu^{II}. It can be inferred that the Zn^{II} ion in the N_3 complex extremely prefers an anionic sulfonamide nitrogen over a neutral primary amino group. It is thus not surprising that Zn^{II} in CA may also have strong affinity to anionic sulfonamides.

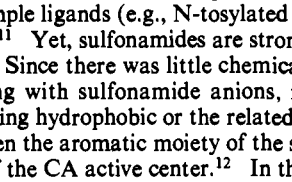

Deprotonation of sulfonamides was reported for Cu^{II} and Pd^{IV} complexes with simple ligands (e.g., N-tosylated amino acid) but rarely for Zn^{II} ion.[11] Yet, sulfonamides are strong CA inhibitors as anionic donors. Since there was little chemical verification of Zn^{II} strong binding with sulfonamide anions, it was often rationalized by invoking hydrophobic or the related complementary interactions between the aromatic moiety of the sulfonamide and nonpolar groups of the CA active center.[12] In the present study,

(8) Zompa, L. J. *Inorg. Chem.* **1978**, *17*, 2531.

(9) A similar UV spectrum change at 225 nm was observed for *p*-toluenesulfonamide (Hts) deprotonation in 10% (v/v) CH_3CN/H_2O at I = 0.10 ($NaClO_4$) and 25 °C, where the pK_a value of 10.5 ± 0.2 is in good agreement with a value of 10.51 ± 0.03 determined by pH titration: ϵ of 9.95 $\times 10^3$ for ts$^-$ (at pH 12.7), 1.14×10^4 for Hts (at pH 7.0).

(10) These IR spectrum changes in SO_2 stretching frequency are in good agreement with that from 1327 cm^{-1} for *p*-toluenesulfonamide (Hts) to 1219 cm^{-1} for sodium *p*-toluenesulfonamidate (Na^+ts^-) in solid state.

(11) Sigel, H.; Martin, R. B. *Chem. Rev.* **1982**, *82*, 420.

Table II. Crystallographic Parameters of **2a**·PF_6

formula	$C_{19}H_{33}N_4O_2F_6PSZn$
formula weight	591.90
cryst syst	orthorhombic
space group	*Pbca*
cryst color	colorless
cell dimens	
a, Å	17.508 (4)
b, Å	15.394 (4)
c, Å	18.377 (5)
V, Å^3	4953 (4)
Z	8
d_{calcd}, g cm^{-3}	1.587
cryst dimens, mm	0.4 × 0.3 × 0.3
radiation	Cu Kα (λ = 1.54178 Å)
μ, cm^{-1}	34.32
temp, K	296 ± 1
scan technique	ω–2θ
scan width, deg	1.10 + 0.3 tan θ
scan speed, deg min^{-1}	32 (in ω)
refinement	full-matrix least-squares
no. of unique reflcns	4135
no. of observed reflcns ($I > 3\sigma(I)$)	2862
R	0.040
R_w	0.056

Table III. Selected Bond Distances (Å), Hydrogen Bond Distances (Å), and Bond Angles (deg) of **2a**·PF_6

Zn–N(1)	2.037 (3)	Zn–N(5)	2.019 (3)
Zn–N(9)	2.018 (4)	Zn–N(16)	1.925 (3)
Zn–O(24)	2.907 (3)	N(16)–S(17)	1.575 (3)
S(17)–O(24)	1.436 (3)	S(17)–O(25)	1.442 (3)
O(25)···HN(9) [$-x, -y, -z$]			2.18 (4)
F(3)···HN(5) [$+x, {}^1/_2 - y, {}^1/_2 + z$]			2.53 (4)
N(1)–Zn–N(5)	105.4 (1)	N(1)–Zn–N(9)	105.5 (1)
N(1)–Zn–N(16)	102.1 (1)	N(5)–Zn–N(9)	99.5 (1)
N(5)–Zn–N(16)	123.2 (1)	N(9)–Zn–N(16)	119.5 (2)
Zn–N(16)–S(17)	117.6 (2)	N(16)–S(17)–O(25)	113.0 (2)
N(16)–S(17)–O(24)	106.7 (2)	N(16)–S(17)–C(18)	106.6 (2)

we have demonstrated the extremely facile deprotonation of the sulfonamide group in **2a** at very low pH < 7 (otherwise pK_a = 11.2, see the previous paragraph) and [Zn^{II}] = [L_2] = 1 mM (see Figure 1b). This fact is certainly due to the proximity of the sulfonamide to Zn^{II}. The complex **2a**, as described later, has no catalytic power for ester hydrolysis. Thus, our new Zn^{II} complex **2a** chemically well-mimics the sulfonamide anion binding to the Zn^{II} in CA. It is also concluded that an effect of the hydrophobic environment may be secondary in inviting aromatic sulfonamides to the CA active center.

An X-ray Crystal Structure of Tosylamidopropyl[12]aneN$_3$ Zn^{II}–Complex, 2a·PF$_6$. Colorless crystals of **2a**·PF_6 for X-ray crystallographic study were obtained by slow evaporation of an aqueous solution at room temperature. The elemental analysis (C, H, N), ^{1}H NMR, and IR data suggested the formula Zn^{II}–L_2·PF_6. The final support for the deprotonated sulfonamide anion coordinating structure **2a** comes from an X-ray crystal analysis. Figure 3 shows an ORTEP drawing of **2a**·PF_6 with 50% probability thermal ellipsoids. Crystal data and data collection parameters are displayed in Table II. Selected interatomic distances, hydrogen bond distances, and bond angles are listed in Table III.

A somewhat distorted tetrahedral Zn^{II} coordination is evident with the [12]aneN$_3$ moiety of three nitrogens N(1), N(5), N(9), and a *unidentate* sulfonamide N$^-$ anion (N(16)). The sulfonamide oxygens O(24) and O(25) seem to have no direct interaction with Zn^{II}; the Zn···O(24) is distant of 2.907 (3) Å and O(25) makes a hydrogen bond with HN(9) of a neighbor molecule (O(25)···HN(9)[$-x, -y, -z$] = 2.18 (4) Å). We thus conclude that the sulfonamide anions need not be bidentate donors, as often proposed to account for their strong affinity to the Zn^{II} in CA.[2c] One F atom of the counter anion PF_6^- binds to a neighboring HN group (F(3)···HN(5) [$+x, {}^1/_2 - y, {}^1/_2 + z$] = 2.53 (4) Å). The Zn^{II}–N$^-$ bond is extremely shortened 1.925 (3) Å, which is shorter than the Zn^{II}–macrocyclic N bond lengths of the average 2.025 Å. Furthermore, this Zn^{II}–N$^-$ bond length is shorter than those of the Zn^{II}–OH$^-$ (1.944 Å) in a tetrahedral Zn^{II}–[12]aneN$_3$ complex **1b**,[5a] the Zn^{II}–O$^-$(phenolate) (1.930 Å) in trigonal bipyramidal Zn^{II}–phenolate–[12]aneN$_3$ complex **8**,[5c] and the Zn^{II}–N(CH$_3$)$_2$ (2.00 Å) in tetrahedral Zn^{II}–dimethylaminopropyl[12]aneN$_3$ complex **9**.[13] These facts are compatible with very strong acid properties of Zn^{II} in favor of sulfonamide N$^-$ anion over neutral nitrogen and O$^-$ anion donors. The crystal structure of **2a** may be viewed as a good model for the tetrahedral Zn^{II} coordination environment of CA with 3-(acetoxymercurio)-4-aminobenzenesulfonamide anion with average Zn^{II}–N$^-$ and Zn^{II}–N(imidazole) distances of ca. 2.0 Å.[3]

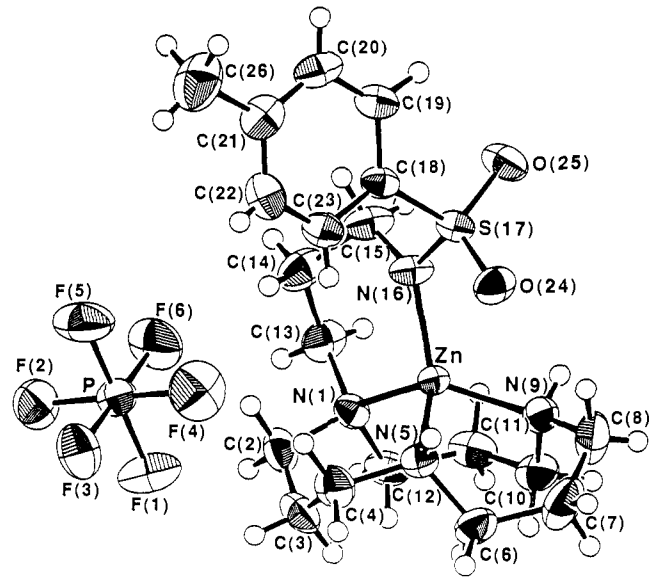

Figure 3. ORTEP drawing (50% probability) of **2a**·PF_6.

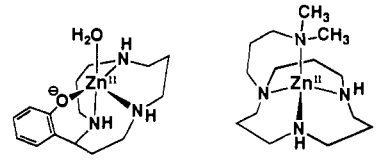

8 **9**

Intermolecular Aromatic Sulfonamide (Haa, Hns, Hts) Affinities to Zn^{II}–[12]aneN$_3$. Recently, we have shown Zn^{II}–OH$^-$ in **1b** to be a good catalyst like CA for 4-nitrophenyl acetate hydrolysis,[5a] whereby common properties are as follows: (i) the Zn^{II}–OH$^-$ species (in **1b** and CA) are strong nucleophiles to attack carbonyl carbon; (ii) anions (e.g., Cl$^-$, CH$_3$COO$^-$) may bind to the Zn^{II} and such complexes are less reactive as the nucleophile; and (iii) the monoanion affinity order for Zn^{II}–[12]aneN$_3$ and CA is common OH$^-$ > CH$_3$COO$^-$ > I$^-$ > Cl$^-$, and the magnitudes of such 1:1 anion complex stability (determined by potentiometric pH titration) for Zn^{II}–[12]aneN$_3$ are almost the same as those for CA.[5a,b] However, the constants for sulfonamide binding to Zn^{II}–[12]aneN$_3$ could not be determined due to insufficient solubilities in the potentiometric pH titration method. We now have succeeded in the sulfonamide affinity measurement by an inhibition kinetic method in the **1b**-promoted NA hydrolysis (Scheme II), which is almost the same technique as Pocker's

(12) (a) Pocker, Y.; Sarkanen, S. *Adv. Enzymol.* **1987**, *47*, 149. (b) Pocker, Y.; Stone, J. T. *Biochemistry* **1967**, *6*, 668. (c) Pocker, Y.; Stone, J. T. *Biochemistry* **1968**, *7*, 2936.

(13) Alcock, N. W.; Benniston, A. C.; Moore, P.; Pike, G. A.; Rawle, S. C. *J. Chem. Soc., Chem. Commun.* **1991**, 706.

Table IV. Comparison of Second-Order NA Hydrolysis Rate Constants, k_i (M^{-1} s^{-1}) at pH 8.40 (50 mM TAPS Buffer), I = 0.10, and 25 °C

promoter	k_i	pK_a
1b	4.1×10^{-2} [a]	7.20[g]
acetazolamide	$(5.7 \pm 0.3) \times 10^{-3}$ [b]	7.48 ± 0.02[h]
p-nitrobenzenesulfonamide	$(1.4 \pm 0.2) \times 10^{-3}$ [c]	9.38 ± 0.02[h]
p-toluenesulfonamide	$(1.6 \pm 0.2) \times 10^{-4}$ [d]	10.51 ± 0.03[h]
2a	$<10^{-4}$ [e]	
HCO_3^-	$(1.8 \pm 0.2) \times 10^{-4}$ [f]	

[a] From ref 5a. [b] Determined at $[Haa]_t$ = 0.5, 1.0, 2.5, 5.0, and 10 mM. [c] Determined at $[Hns]_t$ = 2.5, 5.0, 7.5, and 10 mM. [d] Determined at $[Hts]_t$ = 10, 15, 20, and 25 mM. [e] Determined at [**2a**] = 1.0, 2.0, and 3.0 mM. [f] Determined at $[HCO_3^-]_t$ = 10, 25, 35, and 50 mM. [g] This value (from ref 6) is a coordinate-water deprotonation constant for **1a** in 10% (v/v) CH_3CN aqueous solution at I = 0.10 ($NaClO_4$) and 25 °C. [h] Determined by potentiometric pH titration in 10% (v/v) CH_3CN aqueous solution at I = 0.10 ($NaClO_4$) and 25 °C.

procedure to determine sulfonamide binding to CA.[12b]

The sulfonamides and 4-nitrophenyl acetate are not soluble enough in pure water, so we used CH_3CN as a cosolvent. We first conducted potentiometric pH titrations of 1.0 mM sulfonamides to determine thermodynamic deprotonation constants, 7.48 ± 0.02 for Haa, 9.38 ± 0.02 for Hns, and 10.51 ± 0.03 for Hts at I = 0.10 ($NaClO_4$) and 25 °C.[14] Next we examined whether NA hydrolysis is effected by Haa, Hns, and Hts (at various concentration) by themselves and **2a** (at 1, 2, or 3 mM) at pH 8.40, I = 0.10 and 25 °C in 10% (v/v) CH_3CN aqueous solution. Indeed, these three sulfonamides hydrolyze 4-nitrophenyl acetate with second-order dependence (each first-order for [NA] and [sulfonamide], Table IV) to produce 4-nitrophenolate and acetate. On the other hand, **2a** practically has no effect (<1% activity of **1b**). The near absence of activity for **2a** indicates that the (intramolecular) sulfonamide N^- coordination inhibits formation of the Zn^{II}–OH^- species to act as a nucleophile as **1b**. This is the first chemical model of sulfonamide inhibition in CA catalytic reactions.[15] Earlier, we reported that the phenolate-coordinating Zn^{II}–[12]aneN$_3$ **8** has also no ester hydrolysis activity, which might be the phenol-inhibition model of CA activity.[5a,b]

Then, the intermolecular sulfonamide affinities to Zn^{II}–[12]-aneN$_3$ were determined by **1b**-promoted NA hydrolysis in the presence of Haa, Hns, or Hts at pH 8.40, I = 0.10 and 25 °C in 10% (v/v) CH_3CN aqueous solution. The real first-order rate constants k_r (s^{-1}) are defined as ($k_{obs} - k_0$), where k_0 (s^{-1}) are control values in the absence of Zn^{II}–[12]aneN$_3$ and inhibitor, and k_{obs} (s^{-1}) the observed first-order rate constants (see Experimental Section). These sulfonamides strongly inhibited the hydrolysis as reported in CA-catalyzed NA hydrolysis.[12] Figure 4 shows plots of k_r vs total concentration of acetazolamide ($[I]_t$ = 0 – 10 mM) in the presence of 1.0 mM Zn^{II}–[12]aneN$_3$ (curve (a)) and in the absence of Zn^{II}–[12]aneN$_3$ (line (b)). In curve (a) k_r reaches a minimum value at ca. 2 mM acetazolamide and then increases with increasing concentration of acetazolamide. Dotted line (c) is extrapolated from the k_r values at higher acetazolamide concentrations, which has the same slope as that of line (b). The intersection (at k_r = 0) is 1 mM, which is equal to the total concentration of Zn^{II}–[12]aneN$_3$. These facts lead to the following conclusions: (i) acetazolamide strongly inhibits **1b**-promoted NA hydrolysis; (ii) acetazolamide and Zn^{II}–[12]-aneN$_3$ interact in a 1:1 ratio; and (iii) such a 1:1 Zn^{II}–acetazolamide complex **1c** (Zn^{II}–L_1–I) has no activity in NA hydrolysis (i.e., k_r = 0).

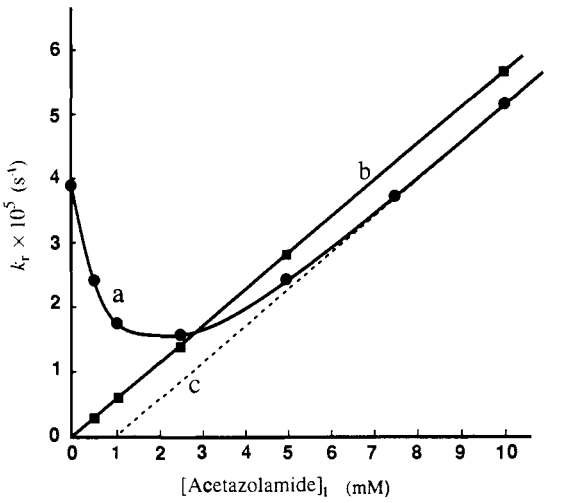

Figure 4. Typical change in k_r (s^{-1}) as a function of total concentration of acetazolamide at I = 0.10 ($NaClO_4$) and pH 8.40 (50 mM TAPS buffer): (a) in the presence of 1.00 mM Zn^{II}–[12]aneN$_3$ and (b) in the absence of Zn^{II}–[12]aneN$_3$. Dashed line (c) is estimated by extrapolation from curve a at >5 mM acetazolamide.

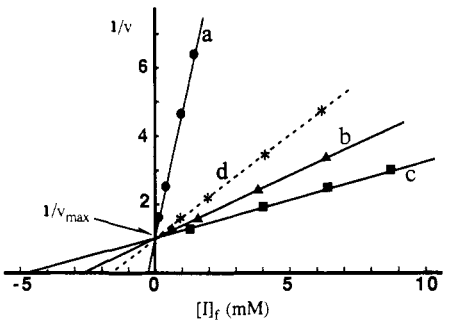

Figure 5. Plots of $1/v$ values as a function of unbinding inhibitor at I = 0.10 ($NaClO_4$) and pH 8.40 (50 mM TAPS buffer): (a) for acetazolamide; (b) for 4-nitrobenzenesulfonamide; (c) for *p*-toluenesulfonamide; and dashed line (d) for HCO_3^-, where $1/v$ are relative values to $1/v_{max}$.

One can calculate concentration of the unbinding inhibitor concentration ($[I]_f$) from eq 3 derived from eq 2, where C_l is total concentration of Zn^{II}–[12]aneN$_3$, C_f total concentration of inhibitor unbinding Zn^{II}–[12]aneN$_3$, and k'_{NA} (= 3.9×10^{-2} M^{-1} s^{-1} at pH 8.4, 25 °C and I = 0.10) observed second-order rate constant for the inhibitor unbinding Zn^{II}–[12]aneN$_3$.

$$k_r = k'_{NA}C_f + k_i[I]_f = k'_{NA}(C_l - [Zn^{II}\text{–}L_1\text{–}I]) + k_i[I]_f \quad (s^{-1}) \quad (2)$$

$$[I]_f = (k_r - k'_{NA}(C_l - [I]_t))/(k'_{NA} + k_i) \quad (M) \quad (3)$$

The following equilibria and eqs 4–9 for K_i, C_f, C_l, k'_{NA}, v_{max}, and v are formulated to determine the apparent affinity constants K_i (M^{-1}) for sulfonamide inhibitors (I), where k_{NA} (= 4.1×10^{-2} M^{-1} s^{-1} at 25 °C and I = 0.10)[5a] is the second-order rate constant for NA hydrolysis promoted by **1b**, v_{max} observed NA hydrolysis rate in the absence of inhibitor, and v observed NA hydrolysis rate in the presence of inhibitor.

$$(\mathbf{1a} + \mathbf{1b}) + I \rightleftharpoons Zn^{II}\text{–}L_1\text{–}I; \quad K_i = [Zn^{II}\text{–}L_1\text{–}I]/C_f[I]_f \quad (M^{-1}) \quad (4)$$

$$C_f = [\mathbf{1a}] + [\mathbf{1b}] \quad (M) \quad (5)$$

$$C_l = C_f + [Zn^{II}\text{–}L_1\text{–}I] \quad (M) \quad (6)$$

$$k'_{NA} = k_{NA}[\mathbf{1b}]/C_f \quad (M^{-1}\ s^{-1}) \quad (7)$$

$$v_{max} = k'_{NA}[NA]C_l \quad (M\ s^{-1}) \quad (8)$$

$$v = k'_{NA}[NA]C_f \quad (M\ s^{-1}) \quad (9)$$

$$1/v = K_i[I]_f/v_{max} + 1/v_{max} \quad (10)$$

(14) The second deprotonation ($aa^- \rightleftharpoons aa^{2-} + H^+$) constant of acetazolamide, 9.06 ± 0.02, was determined by potentiometric pH titration under the same conditions. The composition for sulfonamides at pH 8.40, I = 0.10 and 25 °C is as follows: acetazolamide, Haa (9.0%), aa^- (74.7%), aa^{2-} (16.3%); 4-nitrobenzenesulfonamide, Hns (90.5%), ns^- (9.5%); and *p*-toluenesulfonamide, Hts (99.2%), ts^- (0.8%).

(15) Pocker and Hutson mentioned that CO_2 hydration by a model (pentacoordinate macrocyclic tetraamine–Zn^{II}–OH^- complex) is completely inhibited by acetazolamide (p 215 in ref 12a). However, no details were reported.

Table V. Comparison of Affinity Constants, K_i (M^{-1}) and $K(Zn^{II}L_1-I^-)$ (M^{-1})

	1		
inhibitor	log K_i[a]	log $K(Zn^{II}L_1-I^-)$	CA log K_i[c]
acetazolamide	3.6 ± 0.1	4.9[a]	6.7,[d] 7.9[e]
4-nitrobenzenesulfonamide	2.6 ± 0.1	4.8[a]	7.2[e]
p-toluenesulfonamide	2.4 ± 0.1	5.7[a]	6.3[e]
HCO_3^-	2.8 ± 0.1	4.0[a]	1.6[d]
CH_3COO^-		2.6[b]	1.1[d]
SCN^-		2.4[b]	3.2[d]
Cl^-		1.3[b]	0.7[d]
OH^-		6.4[b]	6.5[d]

[a] Determined by inhibition kinetics at pH 8.4 (50 mM TAPS buffer), I = 0.10 and 25 °C. $K_i = [Zn^{II}-L_1-I]/[\text{inhibitor unbinding } Zn^{II}-L_1][I]_f$ (M^{-1}). $K(Zn^{II}L_1-I^-) = [Zn^{II}-L_1-\text{inhibitor}^-]/[\mathbf{1a}][\text{inhibitor}^-]$ (M^{-1}). [b] Determined by potentiometric pH titration at 25 °C and I = 0.10 in ref 5a. [c] $K_i = [CA-I]/[\text{inhibitor unbinding CA}][I]_f$ (M^{-1}). [d] Determined by inhibition kinetics in CA-promoted NA hydrolysis at pH 8.5 (Tris buffer) from ref 12b. [e] Determined by formation and deassociation kinetics with human carbonic anhydrase at pH 6.5 and 25 °C in ref 2a.

Substitution of eqs 4–8 into eq 9 affords eq 10, where $[I]_f$ is a concentration of the unbinding inhibitor. A plot of $1/v$ against $[I]_f$ has given a straight line with an intercept of $1/v_{max}$ (see Figure 5). From the intersection on the x-axis (i.e., at $1/v = 0$), K_i is given by $-[I]_f^{-1}$. Thus, apparent affinity constant, log K_i = 3.6 ± 0.1 was determined for acetazolamide.

Likewise, the inhibition effects by 4-nitrobenzenesulfonamide and *p*-toluenesulfonamide were measured under the same conditions. The same data treatment with eq 10 gave log K_i = 2.6 ± 0.1 for 4-nitrobenzenesulfonamide and 2.4 ± 0.1 for *p*-toluenesulfonamide.

These K_i values exhibit the same trend as those reported for CA (see Table V),[2a] suggesting that a similar inhibition mechanism is prevailing for our model and CA. However, we saw much greater magnitude of the sulfonamide affinities to CA (log K_i = 7.9 for Haa, 7.2 for Hns, 6.3 for Hts)[2a] than those to our model. These values, however, must be compensated by the noncoordinating sulfonamide affinities, log $K_i \sim 3$ for apo-CA (i.e., Zn^{II}–unbinding CA).[2b,16] Therefore, the intrinsic Zn^{II}–sulfonamide affinity constants may be estimated to be log $K_i \sim 4$, which are closer to the more "intimate" affinity constants derived from our model.

Although there has been controversy on the sulfonamide inhibition mechanism, the deprotonated sulfonamide inhibitors appear to bind to the Zn^{II} in CA.[2] Our present thermodynamic (with **2a**) and kinetic results (with **1c** and **2a**) have proven that sulfonamide hydrogen (normally $pK_a > 10$) can be dissociated at pH as low as ~8 to bind with Zn^{II}. Furthermore, the acidity of Zn^{II} ion in the N_3 ligand field is sufficient to substitute for less acidic protons such as H_2O (to Zn^{II}–OH^-)[5a] and RCONH (to $RCON^- - Zn^{II}$).[5d]

Determination of 4-Nitrobenzenesulfonamide (Hns) Affinity to Zn^{II}–[12]aneN$_3$ by a Spectrophotometric Method. The UV absorption spectra of 4-nitrobenzenesulfonamide (Hns) as a function of pH were reported to determine the sulfonamide pK_a value of 9.3,[2d] which agrees with pK_a value of 9.38 determined by potentiometric pH titration (see Table IV). With an increase in the sulfonamide anion (ns^-) concentration the absorption maximum was red-shifted from 261 to 280 nm with an isosbestic point at 274 nm.[2d] We have thus tested whether the ease of generation of the deprotonated sulfonamide anion in the presence of the Zn^{II} complex fits to the log K_i value (= 2.6) obtained kinetically above. The selected UV absorption changed as the ratio $[Zn^{II}$–[12]-aneN$_3$]/[Hns] changes (0–10) at constant pH 8.4 as shown in Figure 6, where $[Zn^{II}$–[12]aneN$_3$] is 0, 1.0, 2.0, 3.0, 5.0, 7.0 or 10.0 mM, and [Hns] is 1.0 mM. With an increase in the ratio, a similar red-shift of the UV absorption spectra occurred with a decrease in absorption at ca. 260 nm, an increase at ca. 300 nm, and an isosbestic point at 267 nm. From the UV spectral changes at 260 and 300 nm, we could calculate the apparent affinity constant log K_i of 2.7 ± 0.1 for Hns by the same method as described by Connors.[17] This thermodynamically obtained K_i value is in excellent agreement with log K_i = 2.6 determined by the inhibition kinetics. This result supports the sulfonamide binding to Zn^{II}–[12]aneN$_3$ only as an anionic form ns^-. We could then calculate the 4-nitrobenzenesulfonamide anion affinity constant log $K(Zn^{II}L_1-I^-)$ of 4.8 using eq 11 from the pK_a values of Hns and Zn^{II}–[12]aneN$_3$ as well as the K_i value. The similarly calculated log $K(Zn^{II}-L_1-I^-)$ values for Haa and Hts are listed in Table V.

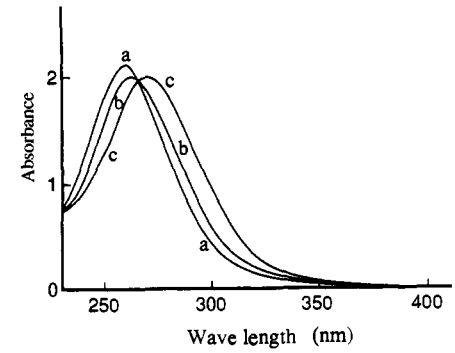

Figure 6. Selected UV absorption spectra of 1.0 mM 4-nitrobenzenesulfonamide at pH 8.40 (50 mM TAPS buffer), I = 0.10 ($NaClO_4$) and 25 °C with 2 mm cell: (a) in the absence of Zn^{II}–[12]aneN$_3$; (b) solution a + 2.0 mM of Zn^{II}–[12]aneN$_3$; and (c) solution a + 10 mM Zn^{II}–[12]aneN$_3$.

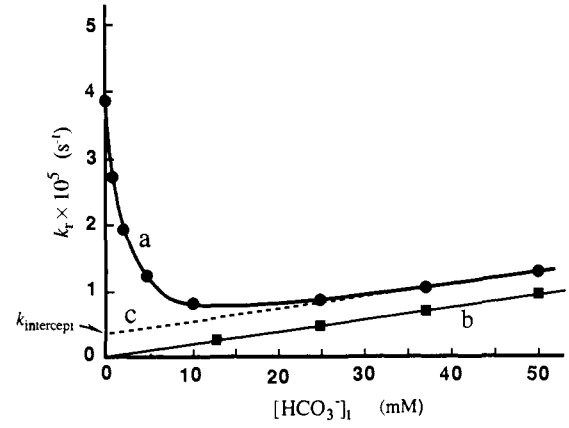

Figure 7. Typical change in k_r (s^{-1}) as a function of total concentration of HCO_3^- at I = 0.10 ($NaClO_4$) and pH 8.40 (50 mM TAPS buffer): (a) in the presence of 1.00 mM Zn^{II}–[12]aneN$_3$ and (b) in the absence of Zn^{II}–[12]aneN$_3$. Dashed line (c) is estimated by extrapolation from curve a at >25 mM HCO_3^-.

1a + inhibitor$^-$ ⇌ **1c**; $K(Zn^{II}L_1-I^-) = [Zn^{II}-L_1-\text{inhibitor}^-]/[\mathbf{1a}][\text{inhibitor}^-]$ (M^{-1}) (11)

A CA–Substrate HCO_3^- Affinity to Zn^{II}–[12]aneN$_3$. Until now, there has been little quantitative data for HCO_3^- binding to CA models. In order to evaluate HCO_3^- affinities to Zn^{II}–[12]aneN$_3$, we have conducted kinetics of **1b**-promoted NA hydrolysis in the presence of excess HCO_3^- at pH 8.40, I = 0.10 and 25 °C in 10% (v/v) CH_3CN aqueous solution, as done above for sulfonamide inhibitions. As anticipated, HCO_3^- strongly inhibited the hydrolysis as the sulfonamides did. Plots of k_r against total concentration of HCO_3^- ($[I]_t$) in the presence of 1.0 mM Zn^{II}–

(16) According to a molecular mechanics study on binding of benzenesulfonamides to CA, about 60% of CA–sulfonamide complex formation energy is contributed by the interaction energy between sulfonamides and Zn^{II}: Menziani, M. C.; Bendetti, P. G. D.; Richards, W. G. *J. Med. Chem.* **1989**, *32*, 951.

(17) Connors, K. A. In *Binding Constants*; John Wiley & Sons: New York, 1987; Chapter 4, p 141.

[12]aneN$_3$ (Figure 7a) and in the absence of Zn^{II}–[12]aneN$_3$ (Figure 7b) are somewhat similar to the same plots for acetazolamide (Figure 4). In curve (a) k_r reaches a minimum value at ca. 10 mM HCO_3^- and then increases with increasing concentration of HCO_3^-. Dotted line (c) extrapolated with the k_r values of line (a) at higher HCO_3^- concentration has an intercept on y-axis ($k_{intercept}$) and the same slope as that of line (b). These results are compatible with (i) HCO_3^- inhibits **1b**-promoted NA hydrolysis; (ii) HCO_3^--bound Zn^{II} complex has a small but finite nucleophilicity toward NA, unlike the sulfonamide anion-bound complex which has no activity in the hydrolysis; (iii) unbinding HCO_3^- also is a weak nucleophile; and (iv) a value of $k_{intercept}$/(total concentration of Zn^{II} complex) gives the second-order rate constant $k_{Zn^{II}L\text{-}I} = (3.5 \pm 0.3) \times 10^{-3}$ M^{-1} s^{-1} for Zn^{II}–$\mathbf{L_1}$–HCO_3^- complex in the hydrolysis. One can calculate the unbinding HCO_3^- concentration ($[I]_f$) from eq 12 instead of eq 2 for sulfonamides. As before, the apparent HCO_3^- affinity constant log K_i of 2.8 ± 0.1 (see dotted line (d) in Figure 5) and real affinity constant log K(Zn^{II}L$_1$–I$^-$) value of 4.0 were determined.

$$k_r = k'_{NA}C_f + k_i[I]_f + k_{ZnL\text{-}I}[Zn^{II}\text{–}\mathbf{L_1}\text{–}I]$$
$$= k'_{NA}(C_t - [Zn^{II}\text{–}\mathbf{L_1}\text{–}I]) + k_i[I]_f + k_{ZnL\text{-}I}[Zn^{II}\text{–}\mathbf{L_1}\text{–}I]\ (s^{-1}) \quad (12)$$

The HCO_3^- affinity to CA is reported to be much smaller with log K_i of 1.6 (pH 8.5 Tris buffer),[12b] while aromatic sulfonamide affinities are much greater log K_i of 6–8.[2a,12b] On the other hand, our value with the model complex Zn^{II}–[12]aneN$_3$ for HCO_3^- affinity (log K_i = 2.8) is in the range for sulfonamide affinities (log K_i of 2.4–3.6). We believe that our values reflect the intrinsic interactions between Zn^{II} and these inhibitors and substrate. In the case of CA, hydrophobic compounds (e.g., aromatic sulfonamides, 4-nitrophenyl acetate) may bind into the hydrophobic pocket more favorably than hydrophilic HCO_3^- before complexing to the Zn^{II}.

Conclusion in Relevance to the CA–Inhibitors or CA–HCO_3^- Interactions. Present results with our model complexes have significant implication in relevance to the specific functions of Zn^{II} in CA. Together with our previous anion affinity data[5a,b] (see Table V) we have now shown for the first time intrinsically very strong affinity of Zn^{II} to HCO_3^- over other biologically relevant anions (Cl$^-$ and CH_3COO^-), which is parallel to CA. The stronger binding of HCO_3^- is rationalized by its higher basicity (i.e., higher pK_a value of 6.0).[18] Because of the stronger affinity toward Zn^{II}, HCO_3^- binding to CA is unhindered by more abundant anion Cl$^-$ at $[HCO_3^-] \sim 27$ mM and $[Cl^-] \sim 105$ mM in blood,[19] which is prerequisite for the HCO_3^- dehydration by CA.

However, the HCO_3^- bound to Zn^{II} (with log K(Zn^{II}L$_1$–I$^-$) = 4.0) can thermodynamically be easily replaced by OH$^-$ generated on Zn^{II} at physiological pH ~ 7 (with log K(Zn^{II}L$_1$–I$^-$) = 6.4), a fact favorable for the catalytic turnover of the CO_2 hydration in CA.

Aromatic sulfonamides effectively compete with HCO_3^- for CA. The apparent binding constants log K_i (at pH 8.4, Table V) with our model are consistent with the previous biochemical facts.[12b] One of the most potent inhibitors, acetazolamide, shows the greatest log K_i of 3.6, which is more than log K_i of 2.8 for HCO_3^-. Interestingly, the more basic p-toluenesulfonamide anion has the largest anion affinity constant log K(Zn^{II}L$_1$–I$^-$) of 5.7. This is not surprising in view of the fact that the acidic nature of the Zn^{II} would prefer strong basic anions. Figure 8, which plots log K(Zn^{II}L$_1$–I$^-$) vs pK_a for the conjugate acids, supports all of our conclusions. Overall, at physiological pH, the ease of formation of the anionic I$^-$ (determined by pK_a) and the Zn^{II}–I$^-$ binding affinities will determine the apparent Zn^{II} inhibitor affinities. These log K_i values may be compared with the reported log K_i for CA. The latter values, however, may comprise bindings (e.g., hydrophobic interaction, hydrogen bondings) other than Zn^{II}–I$^-$ intrinsic interaction.

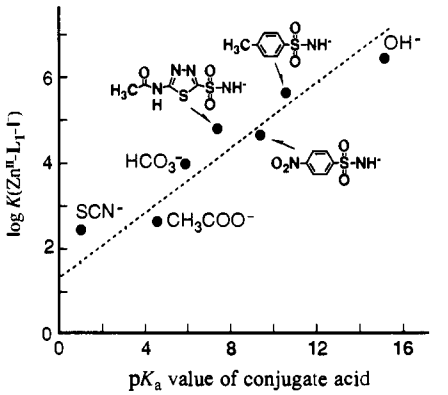

Figure 8. Plots of the monoanion affinity constants, log K(Zn^{II}L$_1$–I$^-$) against pK_a values for the conjugate acid.

Experimental Section

General Information. All reagents and solvents used were of analytical grade. Acetonitrile (CH_3CN) was distilled over calcium hydride. 4-Nitrophenyl acetate, acetazolamide, 4-nitrobenzenesulfonamide, and p-toluenesulfonamide were recrystallized from dry diethyl ether, H_2O, CH_3CN, and H_2O/EtOH, respectively. Crystalline Zn^{II} complex with $\mathbf{L_1}$ ($\mathbf{1b}_3$·$(ClO_4)_3$·$HClO_4$) was prepared using the same method described previously.[5a] IR and UV spectra were recorded on a Shimadzu FTIR-4200 and a Hitachi U-3200 spectrophotometer, respectively. Melting points were determined by using a Yanaco micro melting apparatus without any corrections. Thin-layer chromatography (TLC) was carried out on Merck Art. 5554 (silica gel) TLC plates. ^{1}H (400 MHz) and ^{13}C NMR (100 MHz) spectra were recorded on a JEOL GX-400 spectrometer at 25.0 ± 0.5 °C, where the ionic strength of the sample was not adjusted. 3-(Trimethylsilyl)propionic-*2,2,3,3-d*$_4$ acid sodium salt (Merck) in D_2O and tetramethylsilane (Merck) in organic solvent were used as internal references.

Synthesis of 1-(3-Aminopropyl)-1,5,9-triazacyclododecane, L$_3$. A solution of 2,4-dioxo-1,5,9-triazacyclododecane (**4**)[7] (3.0 g, 15 mmol) in 150 mL of acrylonitrile was heated at reflux in the dark for 3 days (see Scheme I). After evaporating the remaining acrylonitrile, the residue was crystallized from EtOH to give 9-(2-cyanoethyl)-2,4-dioxo-1,5,9-triazacyclododecane (**5**) as colorless needles (3.58 g, 94% yield): mp 163–164 °C; IR (KBr pellet) 3345, 2959, 2855, 2313 (CN), 1670 (CO), 1631 (CO), 1557, 1455, 1298, 1092, 1060, 951, 721, 588 cm^{-1}; TLC (eluent; CH_2Cl_2–MeOH, 5:1) R_f 0.7; ^{1}H NMR ($CDCl_3$) δ 1.79 (4 H, m, CCH_2C), 2.56–2.60 (4 H, m, NCH_2), 2.59 (2 H, t, J = 6 Hz, NCH_2), 2.73 (2 H, t, J = 6 Hz, CH_2CN), 3.18 (2 H, s, $COCH_2CO$), 3.43 (4 H, quartet, $CONCH_2$), 7.12 (2 H, br, CONH). Anal. Calcd for $C_{12}H_{20}N_4O_2$: C, 57.12; H, 7.99; N, 22.21. Found: C, 57.50; H, 8.02; N, 22.48.

The obtained macrocycle **5** (200 mg, 0.79 mmol) was added to a solution of freshly distilled BH_3–THF (10 mmol) in 50 mL of dry THF at 0 °C.[20] The solution was stirred at room temperature for 1 h and then heated at reflux for 1 day. After decomposition of the excess amount of BH_3 with 6 M aqueous HCl at 0 °C, the solvent was evaporated. The residue was passed through an anion exchange column of Amberlite IRA-400 with water to obtain 1-(3-aminopropyl)-1,5,9-triazacyclododecane, L$_3$, as yellow oil. Crystallization of the oil from 48% aqueous HBr/EtOH afforded tetrahydrobromide salt (L$_3$·4HBr) as colorless crystals in 71% yield (312 mg): IR (KBr pellet) 3432, 2998, 2625, 1580, 1460, 1427, 1071 cm^{-1}; TLC (eluent; CH_2Cl_2–MeOH–28% aqueous NH_3, 2:2:1) R_f 0.2; ^{1}H NMR (D_2O) δ 1.86–1.93 (6 H, m, CCH_2C), 2.04 (2 H, m, CCH_2CNH_2), 2.75 (2 H, t, J = 6 Hz, NCH_2), 2.83 (4 H, t, J = 6 Hz, NCH_2), 3.02 (2 H, t, J = 8 Hz, NCH_2), 3.12 (4 H, t, J = 6 Hz, NCH_2), 3.18 (4 H, t, J = 6 Hz, NCH_2). Anal. Calcd for $C_{12}H_{28}N_4$·4HBr·0.5H_2O: C, 25.69; H, 5.93; N, 9.99. Found: C, 25.60; H, 5.89; N, 10.07.

Synthesis of 1-(3-p-Toluenesulfonamidopropyl)-1,5,9-triazacyclododecane, HL$_2$. L$_3$·4HBr (1.5 g, 2.7 mmol) was passed through an anion exchange column of Amberlite IRA-400 with water to get the acid free form of L$_3$. The resulting acid-free L$_3$ and $^1/_3$ equiv of L$_3$·4HBr (0.5 g, 0.89 mmol) (so that overall L$_3$·HBr is present) were added into a $CHCl_3$

(18) Martell, A. E.; Smith, R. M. *Critical Stability Constants*; Plenum: New York.

(19) Smith, E. L.; Hill, R. L.; Lehman, I. R.; Lefkowitz, R. J.; Handler, P.; White, A. In *Principles of Biochemistry, Mammalian Biochemistry*; McGraw-Hill International Book Co.: Japan, 1983; p 5.

(20) Kimura, E.; Kotake, Y.; Koike, T.; Shionoya, M.; Shiro, M. *Inorg. Chem.* **1990**, *29*, 4991.

solution (5 mL) of triethylamine (740 mg, 7.2 mmol). A solution of *p*-toluenesulfonyl chloride (700 mg, 3.6 mmol) in 2 mL of $CHCl_3$ was added dropwise to the reaction mixture for 30 min at −10 °C and then stood for 12 h at 5 °C. The reaction mixture was poured into 30 mL of ice-cold water. The aqueous solution was extracted with three 30-mL portions of CH_2Cl_2. After evaporating the solvent, the residue was recrystallized from a mixture of concentrated HCl solution and EtOH to obtain colorless crystals of $HL_2{\cdot}3HCl{\cdot}1.5H_2O$ in 77% yield (1.42 g) (see Scheme I): IR (KBr pellet) 3440, 2938, 2789, 1584, 1478, 1458, 1431, 1323, 1306, 1159, 1094, 816, 664 cm^{-1}; TLC (silica gel, eluent 10% aqueous NaCl/EtOH = 1:1) R_f 0.7; ^1H NMR (D_2O) δ 1.68 (2 H, m, CCH_2CNS), 1.86 (4 H, quintet, J = 6 Hz, CCH_2C), 1.95 (2 H, quintet, J = 6 Hz, CCH_2C), 2.45 (3 H, s, CH_3), 2.71 (2 H, t, J = 6 Hz, NCH_2), 2.81 (4 H, t, J = 6 Hz, NCH_2), 2.97 (2 H, t, J = 7 Hz, CH_2NS), 3.02 (4 H, t, J = 6 Hz, NCH_2), 3.10 (4 H, t, J = 6 Hz, NCH_2), 7.50 (2 H, d, J = 8 Hz, ArH), 7.78 (2 H, d, J = 8 Hz, ArH); ^{13}C NMR (D_2O) δ 148.1, 137.6, 133.0, 129.6, 55.1, 50.3, 45.0, 44.1, 42.5, 26.7, 23.5, 23.4, 20.6. Anal. Calcd for $C_{19}H_{34}N_4O_2S{\cdot}3HCl{\cdot}1.5H_2O$: C, 43.97; H, 7.77; N, 10.80. Found: C, 43.93; H, 7.40; N, 10.65.

Synthesis of Tosylamidopropyl[12]aneN$_3$–Zinc(II) Complex, 2a·PF$_6$. $ZnBr_2$ (93 mg, 0.4 mmol) and KPF_6 (0.8 mmol) were dissolved in an aqueous solution (10 mL) of $HL_2{\cdot}3HCl{\cdot}1.5H_2O$ (200 mg, 0.4 mmol). The solution pH was adjusted to 7.5 with aqueous 1 M NaOH. The resulting white powder was filtered and then recrystallized from water. Colorless crystals of **2a**·PF_6 were obtained in 60% yield: IR (KBr pellet) 3447, 3285, 3235, 2936, 1456, 1397, 1264, 1146, 1127, 1090, 1024, 878, 845, 666, 600, 559 cm^{-1}. ^1H NMR (D_2O, pD 7.5) δ 1.76–2.13 (8 H, m, CCH_2C), 2.44 (3 H, s, CH_3), 2.84 (2 H, t, J = 5 Hz, CH_2NS), 2.89–3.03 (10 H, m, CH_2N), 3.25–3.32 (4 H, m, CH_2N), 7.45 (2 H, d, J = 8 Hz, ArH), 7.71 (2 H, d, J = 8 Hz, ArH); ^{13}C NMR (D_2O, pD 7) δ 188.7, 139.1, 132.8, 129.6, 61.6, 61.4, 53.8, 53.4, 48.7, 28.7, 27.2, 27.0, 23.4. Anal. Calcd for $C_{19}H_{33}N_4O_2SZn{\cdot}PF_6$: C, 38.55; H, 5.62; N, 9.47. Found: C, 38.36; H, 5.59; N, 9.50.

Synthesis of Tosylamidopropyl[12]aneN$_3$–Copper(II) Complex, 2b·BPh$_4$. $CuCl_2{\cdot}2H_2O$ (50 mg, 0.3 mmol) was dissolved in an aqueous solution (15 mL) of $HL_2{\cdot}3HCl{\cdot}1.5H_2O$ (140 mg, 0.3 mmol) at room temperature. The solution pH was adjusted to 10 with aqueous 1 M NaOH, where the solution color chaged to green. After filtering the solution through a membrane filter (cellulose nitrate, 0.45 μm pore size), an aqueous solution (5 mL) of sodium tetraphenylborate ($NaBPh_4$, 0.9 mmol) was added to the filtrate. The resulting fine green crystals of **2b**·$BPh_4{\cdot}H_2O$ were filtered and then washed with 3 mL of distilled water: yield 95%; IR (KBr pellet) 3472, 3256, 3056, 2928, 2863, 1580, 1478, 1427, 1267, 1132, 1092, 1085, 1020, 868, 735, 708, 664, 613 cm^{-1}; UV and visible absorption in aqueous solution at I = 0.10 ($NaClO_4$), pH 8 and 25 °C; 396 nm (ϵ 1400), 635 nm (ϵ 250). Anal. Calcd for $C_{43}H_{53}N_4O_2SCu{\cdot}H_2O$: C, 66.02; H, 7.09; N, 7.16. Found: C, 65.64; H, 6.84; N, 7.28.

Synthesis of Aminopropyl[12]aneN$_3$–Zinc(II) Complex, 3a·(ClO$_4$)$_2$. $Zn(ClO_4)_2{\cdot}6H_2O$ (350 mg, 0.9 mmol) and $NaClO_4$ (4.4 mmol) were dissolved in an aqueous solution (10 mL) of $L_3{\cdot}4HCl$ (480 mg, 0.9 mmol). The solution pH was adjusted to 8.7 with aqueous 1 M NaOH. Colorless crystals of **3a**·$(ClO_4)_2$ were obtained by slow evaporation (ca. 1 week) in 60% yield: IR (KBr pellet) 3440, 3168, 3120, 2934, 1625, 1561, 1466, 1283, 1249, 1144, 1117 cm^{-1}; ^1H NMR (D_2O, pD 8.5) δ 1.69–2.21 (8 H, m, CCH_2C), 2.91–3.03 (10 H, m, CH_2N), 3.13 (2 H, t, J = 5 Hz, CH_2N), 3.22–3.32 (4 H, m, CH_2N); ^{13}C NMR (D_2O, pD 8) δ 61.6, 60.0, 53.2, 52.3, 45.4, 28.2, 27.4, 25.7. Anal. Calcd for $C_{12}H_{28}N_4Zn{\cdot}(ClO_4)_2$: C, 29.26; H, 5.73; N, 11.37. Found: C, 29.33; H, 5.78; N, 11.43.

Potentiometric pH Titrations. The preparation of the test solutions and the calibration of the electrode system (Orion Research 811 pH meter and Orion 91-02 electrode with 90-0019 reference electrode filling solution) were described earlier.[21] All samples were kept under argon (>99.999% purity) atmosphere, and the solution temperature was maintained at 25.0 ± 0.1 °C. The calculation methods for the protonation constants of the ligands and metal complexation constants are the same as described previously.[5d,22] For the determination of these constants, at least three independent titrations were always made. The protonation constants K_n are defined as $[H_nL]/[H_{n-1}L]{\cdot}a_{H^+}$, and the 1:1 metal complexation constants $K(ML)$ are $[ML]/[M][L]$. The pH value in 10% (v/v) CH_3CN aqueous solution at I = 0.10 ($NaClO_4$) and 25 °C was determined by subtracting 0.03 units from the pH meter reading,[6] where K_w' (= $[H^+][OH^-]$) of $10^{-13.97}$ and f_{H^+} of 0.85 were used.

NMR Measurements. Solutions of L_2 (10 mM) for ^1H NMR pD titration were made up in D_2O (99.9 atom % D from Aldrich), and the pD (= 5.6, 8.0, 10.5, 10.8, 11.2, 11.6, 12.2, 12.5, and 13.2) was adjusted with NaOD (Merck). The pD value was corrected for a deuterium isotope effect using pD = [pH-meter reading] + 0.40.[23] The determination of the microscopic protonation constants of L_2 is the same as described in Geraldes's procedure for pendantless macrocyclic triamines.[24] The first (for the macrocyclic nitrogens) and second protonation constants (for sulfonamide anion) of L_2 can be assigned by following the chemical shifts of the macrocyclic methylene protons or the methyl and aromatic protons, respectively, as a function of pD. Typical ^1H NMR signals (δ) of L_2 at pD 13.2 (10.5) are assigned as follows: ArH 7.67 (7.79), 7.38 (7.50); $NDCH_2$ 2.56 (2.86), 2.53 (2.73); CH_3 2.39 (2.44).

Crystallographic Study. A colorless crystal with dimensions 0.4 × 0.3 × 0.3 mm of **2a**·PF_6 was used for data collection. The lattice parameters and intensity data were measured on a Rigaku AFC5R diffractometer with graphite monochromated Cu Kα radiation and a 12 KW rotating anode generator. The structure was solved by direct method, and the non-hydrogen atoms were refined anisotropically. The final cycle of full-matrix least-squares refinement was based on 2862 observed reflections to give R = 0.040 and R_w = 0.056. All calculations were performed using the TEXSAN crystallographic software package developed by Molecular Structure Corporation (1985).

Kinetics of 4-Nitrophenyl Acetate Hydrolysis. The hydrolysis (or 4-nitrophenolate release reaction) rate of 4-nitrophenyl acetate (NA) was measured by an initial slope method (following the increase in 400-nm absorption of 4-nitrophenolate) in 10% (v/v) CH_3CN aqueous solution at 25.0 ± 0.5 °C, as previously described for **1b**-promoted NA hydrolysis.[5a] Buffered solutions containing 50 mM TAPS buffer at pH 8.40 were used, and the ionic strength was adjusted to 0.10 with $NaClO_4$ (ca. 50 mM). The typical procedure was as follows: After NA (0.50, 1.0, or 2.0 mM) and **1** (1.0 or 2.0 mM) in the presence of inhibitor (0.50–10.0 mM acetazolamide, 1.0–10.0 mM 4-nitrobenzenesulfonamide, 1.0–25.0 mM *p*-toluenesulfonamide, or 1.0–50.0 mM HCO_3^-) were mixed in the buffered solution, the UV absorption decay was recorded immediately and was followed generally until ca. 2% formation of 4-nitrophenolate, where log ϵ of 4-nitrophenolate was 4.24 at 400 nm. The observed rate constants k_{obs} (s^{-1}) were calculated by determining slope of the decay. These inhibitors by themselves promote the ester hydrolysis (e.g., line (b) in Figure 4). Accordingly, we also determined second-order rate constants k_i (M^{-1} s^{-1}) for the inhibitors per se in 10% (v/v) CH_3CN aqueous solution by the same initial slope method as used for **1b**.[5a] All experiments were run in triplicate, and tabulated data represent the average of these experiments. Rate constants were reproducible to ±5%.

Acknowledgment. We are thankful to the Ministry of Education, Science and Culture in Japan for the financial support by a Grant-in-Aid for Encouragement of Young Scientists (No. 03857311) and for Scientific Research on Priority Areas "Bioinorganic Chemistry" (No. 03241105). T.K. expresses his appreciation to Dr. Vincent L. Capuano for his continuous interest and support.

Supplementary Material Available: Tables of atomic coordinates, equivalent isotropic temperature factors, and anisotropic temperature factors for **2a**·PF_6 (5 pages); listing of observed and calculated structure factors for **2a**·PF_6 (20 pages). Ordering information is given on any current masthead page.

(21) Kimura, E.; Koike, T.; Uenishi, K.; Hediger, M.; Kuramoto, M.; Joko, S.; Arai, Y.; Kodama, M.; Iitaka, Y. *Inorg. Chem.* **1987**, *26*, 2975.

(22) Kimura, E.; Yamaoka, M.; Morioka, M.; Koike, T. *Inorg. Chem.* **1986**, *25*, 3883.

(23) Glasoe, P. K.; Long, F. A. *J. Phys. Chem.* **1960**, *64*, 188.

(24) Geraldes, C. F. G. C.; Sherry, A. D.; Marques, M. P. M.; Alpoim, M. C.; Cortes, S. *J. Chem. Soc., Perkin Trans. 2*, **1991**, 137.